

## Electronic Supplementary Information

# Reaction of H + HONO in solid *para*-hydrogen: infrared spectrum of •ONH(OH)

Karolina Anna Haupa<sup>\*a</sup> and Yuan-Pern Lee<sup>\*ab</sup>

<sup>a</sup>*Department of Applied Chemistry and Institute of Molecular Sciences, National Chiao Tung University, 1001 Ta-Hsueh Road, Hsinchu 30010, Taiwan, E-mail: (KAH) [karolina.haupa@gmail.com](mailto:karolina.haupa@gmail.com) (YPL) [yplee@mail.nctu.edu.tw](mailto:yplee@mail.nctu.edu.tw), Tel: +886-3-5131459*

<sup>b</sup> *Institute of Molecular Sciences, Academia Sinica, Taipei 10617, Taiwan*

### Tables and Figures in the ESI

Comparison of vibrational wavenumbers ( $\text{cm}^{-1}$ ) of *trans*- and *cis*-HONO in various matrices and in the gaseous phase is presented in Table S1. Comparison of vibrational wavenumbers ( $\text{cm}^{-1}$ ) of *trans*- and *cis*-DONO and *trans*- and *cis*-HO<sup>15</sup>NO in solid *p*-H<sub>2</sub> is presented in Table S2. Harmonic wavenumbers ( $\text{cm}^{-1}$ ) of HN(OH)<sub>2</sub>, HN(OH)OD, and H•<sup>15</sup>N(OH)<sub>2</sub>, and isotopic ratios D/H and <sup>15</sup>N/<sup>14</sup>N of HN(OH)<sub>2</sub> calculated with the B3LYP/aug-cc-pVTZ method are presented in Table S3; those of •N(OH)<sub>2</sub> and HN(OH)<sub>2</sub> are presented in Tables S4 and S5, respectively. Harmonic wavenumbers ( $\text{cm}^{-1}$ ) of •ONH(OH), •ONH(OD), and •O<sup>15</sup>NH(OH), and isotopic ratios D/H and <sup>15</sup>N/<sup>14</sup>N of •ONH(OH) calculated with the B3LYP/aug-cc-pVTZ method are presented in Table S4; those of •N(OH)<sub>2</sub> are presented in Tables S4 and S5, respectively.

Spectra in the  $\nu_3$  region of H<sub>2</sub>O recorded at various stages of an experiment is presented in Fig. S1. Partial spectra of a HONO/NH<sub>3</sub>/Cl<sub>2</sub>/*p*-H<sub>2</sub> matrix recorded at various stages of an experiment are presented in Fig. S2; those of matrices DONO/NH<sub>3</sub>/*p*-H<sub>2</sub> and HO<sup>15</sup>NO/NH<sub>3</sub>/*p*-H<sub>2</sub> are presented in Figs. S3 and S4, respectively. Geometries of a less stable conformer of •N(OH)<sub>2</sub> optimized with the B3LYP/aug-cc-pVTZ method is shown in Fig. S5.

**Table S1** Comparison of vibrational wavenumbers ( $\text{cm}^{-1}$ ) of *trans*- and *cis*-HONO in various matrices and in the gaseous phase.

mode	<i>trans</i> -HONO						<i>cis</i> -HONO					
	<i>p</i> -H <sub>2</sub>	Ar	Kr	N <sub>2</sub>	gas	<i>p</i> -H <sub>2</sub>	Ar	Kr	N <sub>2</sub>	gas		
$\nu_1$	3574.5 /3568.5	3572.6	3551.1	3558.0	3590.7	3417.7	3412.4 /3410.7		3399.7	3410.0	3426.0	
$\nu_2$	1692.0 /1688.0	1689.1	1684.0	1684.0	1689.0	1635.8	1634.0 /1632.8		1629.0	1633.0	1640.5	
$\nu_3$	1264.9 /1263.9	1265.8	1265.3	1298.0	1266.0	-	-	1315.2	-	1302.0		
$\nu_4$	792.7 /796.6	800.4	794.5	815.0	800.0	850.2	853.1 /850.2	851.9	865.0	851.9		
$\nu_5$	609.5	608.7	606.7	625.0	609.0	606.2	608.0	616.6	-	609.0		
$\nu_6$	551.8	549.4	549.1	583.0	549.4	641.8	638.4	635.0	658.0	639.8		
ref.	this work	<i>a</i>	<i>b</i>	<i>c</i>	<i>d</i>	this work	<i>a</i>	<i>b</i>	<i>c</i>	<i>d</i>		

<sup>a</sup> I. Kleiner, J. Guilmot, M. Carleer and M. Herman, *J. Mol. Spectrosc.*, 1991, **149**, 341–347.

<sup>b</sup> Z. Mielke, K. G. Tokhadze, Z. Latajka and E. Ratajczak, *J. Phys. Chem.*, 1996, **100**, 539–545.

<sup>c</sup> R. T. Hall and G. C. Pimentel, *J. Chem. Phys.*, 1963, **38**, 1889–1897.

<sup>d</sup> L. Khriachtchev, J. Lundell, E. Isoniemi and M. Rasanen, *J. Chem. Phys.*, 2000, **113**, 4265–4273.

**Table S2** Comparison of vibrational wavenumbers ( $\text{cm}^{-1}$ ) of *trans*- and *cis*-DONO and *trans*- and *cis*- $\text{HO}^{15}\text{NO}$  in solid *p*- $\text{H}_2$ .

mode	<i>trans</i> -DONO	<i>cis</i> -DONO	<i>trans</i> - $\text{HO}^{15}\text{NO}$	<i>cis</i> - $\text{HO}^{15}\text{NO}$
$\nu_1$	2638.9	2527.3	3574.5	3417.1
$\nu_2$	1686.0	1621.8	1662.2	1607.8
$\nu_3$	1013.4	-	1264.7	-
$\nu_4$	741.4	811.3	776.5	~833
$\nu_5$	592.5	593.0	598.4	595.0
$\nu_6$	508.6	-	552.3	-

**Table S3** Harmonic wavenumbers ( $\text{cm}^{-1}$ ) of  $\text{HN(OH)}_2$ ,  $\text{HN(OH)OD}$ , and  $\text{H}\bullet^{15}\text{N(OH)}_2$ , and isotopic ratios D/H and  $^{15}\text{N}/^{14}\text{N}$  of  $\text{HN(OH)}_2$  calculated with the B3LYP/aug-cc-pVTZ method.

mode	$\text{HN(OH)}_2$	$\text{HN(OH)OD}$	$\text{H}^{15}\text{N(OH)}_2$	D/H	$^{15}\text{N}/^{14}\text{N}$	PED (%) <sup>a</sup>
$\nu_1$	3790 (56)	3789 (46)	3790 (56)	1.000	1.000	$\nu\text{O1-H2}$ (50) + $\nu\text{O2-H3}$ (50)
$\nu_2$	3789 (35)	2761 (26)	3789 (36)	0.729	1.000	$\nu\text{O1-H2}$ (50) + $\nu\text{O2-H3}$ (50)
$\nu_3$	3482 (6)	3482 (7)	3474 (6)	1.000	0.998	$\nu\text{N-H1}$ (100)
$\nu_4$	1539 (0)	1530 (2)	1539 (0)	0.994	1.000	$\delta\text{H1-N-O4}$ (83)
$\nu_5$	1466 (5)	1409 (23)	1460 (6)	0.961	0.996	$\delta\text{H2-O1-N}$ (36) + $\delta\text{H3-O2-N}$ (36) + $\gamma\text{N-O2-O1-H1}$ (26)
$\nu_6$	1310 (80)	1195 (78)	1308 (84)	0.912	0.999	$\delta\text{H2-O1-N}$ (41) + $\delta\text{H3-O2-N}$ (41) + $\delta\text{H1-N-O}_2$ (16)
$\nu_7$	1145 (106)	993 (47)	1143 (105)	0.867	0.999	$\gamma\text{N-O2-O1-H1}$ (49) + $\delta\text{H2-O1-N}$ (13) + $\delta\text{H3-O2-N}$ (13)
$\nu_8$	930 (2)	909 (6)	913 (2)	0.977	0.981	$\nu\text{O1-N}$ (38) + $\nu\text{O2-N}$ (38) + $\gamma\text{N-O2-O1-H1}$ (14) + $\delta\text{O1-N-O}_2$ (10)
$\nu_9$	861 (201)	859 (203)	844 (192)	0.998	0.981	$\nu\text{O1-N}$ (49) + $\nu\text{O2-N}$ (49)
$\nu_{10}$	530 (1)	528 (3)	527.4 (1)	0.997	0.995	$\delta\text{O1-N-O}_2$ (86)
$\nu_{11}$	440 (127)	400 (96)	439.2 (127)	0.908	0.998	$\tau\text{H2-O1-N-O}_2$ (50) + $\tau\text{H1-O2-N-O1}$ (50)
$\nu_{12}$	305 (35)	250 (24)	304.9 (35)	0.820	1.000	$\tau\text{H2-O1-N-O}_2$ (49) + $\tau\text{H1-O2-N-O1}$ (49)

<sup>a</sup> Calculated by VEDA 4f software. Vibrations with contribution >10% are included; the coefficients are listed in parentheses.

<sup>b</sup> Mode description:  $\nu$ : stretch;  $\delta$ : bend;  $\gamma$ : out-of-plane deformation ;  $\tau$ : torsion.

<sup>c</sup> Calculated IR intensities in  $\text{km mol}^{-1}$  are given in parenthesis.

**Table S4** Harmonic wavenumbers ( $\text{cm}^{-1}$ ) of  $\bullet\text{ONH(OH)}$ ,  $\bullet\text{ONH(OD)}$ , and  $\bullet\text{O}^{15}\text{NH(OH)}$ , and isotopic ratios D/H and  $^{15}\text{N}/^{14}\text{N}$  of  $\bullet\text{ONH(OH)}$  calculated with the B3LYP/aug-cc-pVTZ method.

mode	$\bullet\text{ONH(OH)}$	$\bullet\text{ONH(OD)}$	$\bullet\text{O}^{15}\text{NH(OH)}$	D/H	$^{15}\text{N}/^{14}\text{N}$
$v_1$	3729.4 (67) <sup>a</sup>	2714.2 (38) <sup>a</sup>	3729.4 (68) <sup>a</sup>	0.728	1.000
$v_2$	3369.3 (3)	3369.6 (4)	3361.6 (3)	1.000	0.998
$v_3$	1506.7 (55)	1443.6 (31)	1494.1 (41)	0.958	0.992
$v_4$	1411.6 (66)	1411.0 (74)	1403.2 (78)	1.000	0.994
$v_5$	1285.9 (6)	1080.0 (17)	1276.4 (7)	0.840	0.993
$v_6$	942.0 (188)	899.6 (162)	931.3 (179)	0.955	0.989
$v_7$	761.7 (123)	759.6 (114)	751.7 (123)	0.997	0.987
$v_8$	544.0 (13)	510.4 (16)	540.8 (13)	0.938	0.994
$v_9$	239.6 (126)	185.7 (81)	239.1 (126)	0.775	0.998

<sup>a</sup> Calculated IR intensities in  $\text{km mol}^{-1}$  are given in parenthesis.

**Table S5** Harmonic wavenumbers ( $\text{cm}^{-1}$ ) of  $\bullet\text{N(OH)}_2$ ,  $\bullet\text{N(OH)OD}$ , and  $\bullet^{15}\text{N(OH)}_2$ , and isotopic ratios D/H and  $^{15}\text{N}/^{14}\text{N}$  of  $\bullet\text{N(OH)}_2$  calculated with the B3LYP/aug-cc-pVTZ method.

mode	$\bullet\text{N(OH)}_2$	$\bullet\text{N(OH)OD}$	$\bullet^{15}\text{N(OH)}_2$	D/H	$^{15}\text{N}/^{14}\text{N}$
$\nu_1$	3779.0 (101) <sup>a</sup>	3660.1 (40) <sup>a</sup>	3779.0 (101) <sup>a</sup>	0.969	1.000
$\nu_2$	3659.9 (38)	2751.6 (56)	3659.9 (38)	0.752	1.000
$\nu_3$	1436.7 (65)	1412.6 (58)	1426.9 (70)	0.983	0.993
$\nu_4$	1323.1 (63)	1139.2	1320.6 (62)	0.861	0.998
$\nu_5$	1040.5 (172)	976.4 (166)	1025.9 (156)	0.938	0.986
$\nu_6$	960.6 (63)	906.1 (8)	944.8 (70)	0.943	0.984
$\nu_7$	570.8 (23)	552.3 (25)	567.8 (22)	0.968	0.995
$\nu_8$	343.7 (8)	299.6 (18)	342.7 (8)	0.872	0.997
$\nu_9$	224.3 (221)	192.8 (154)	3779.0 (101)	0.969	1.000

<sup>a</sup> Calculated IR intensities in  $\text{km mol}^{-1}$  are given in parenthesis.

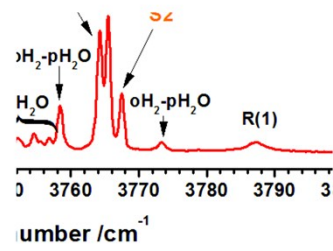


**Fig. S1** Spectra in the  $\nu_3$  region of  $\text{H}_2\text{O}$  recorded at various stages of an experiment. (a) Spectra of a  $\text{HONO}/\text{NH}_3/\text{p-H}_2$  matrix recorded after irradiation at 365 nm for 10 min. (b) Spectra of the same matrix recorded 6 h in darkness after irradiation. The assignments according to S. Tam and M. E. Fajadro (*Low Temp. Phys.*, 2000, **26**, 653-660) and K. A. Kufeld *et al.* (*J. Phys. Chem. Lett.*, 2012, **3**, 342-347) are indicated. Lines marked S1 and S2 are satellite lines of R(0); see text. Red arrows indicate their changes in intensity.

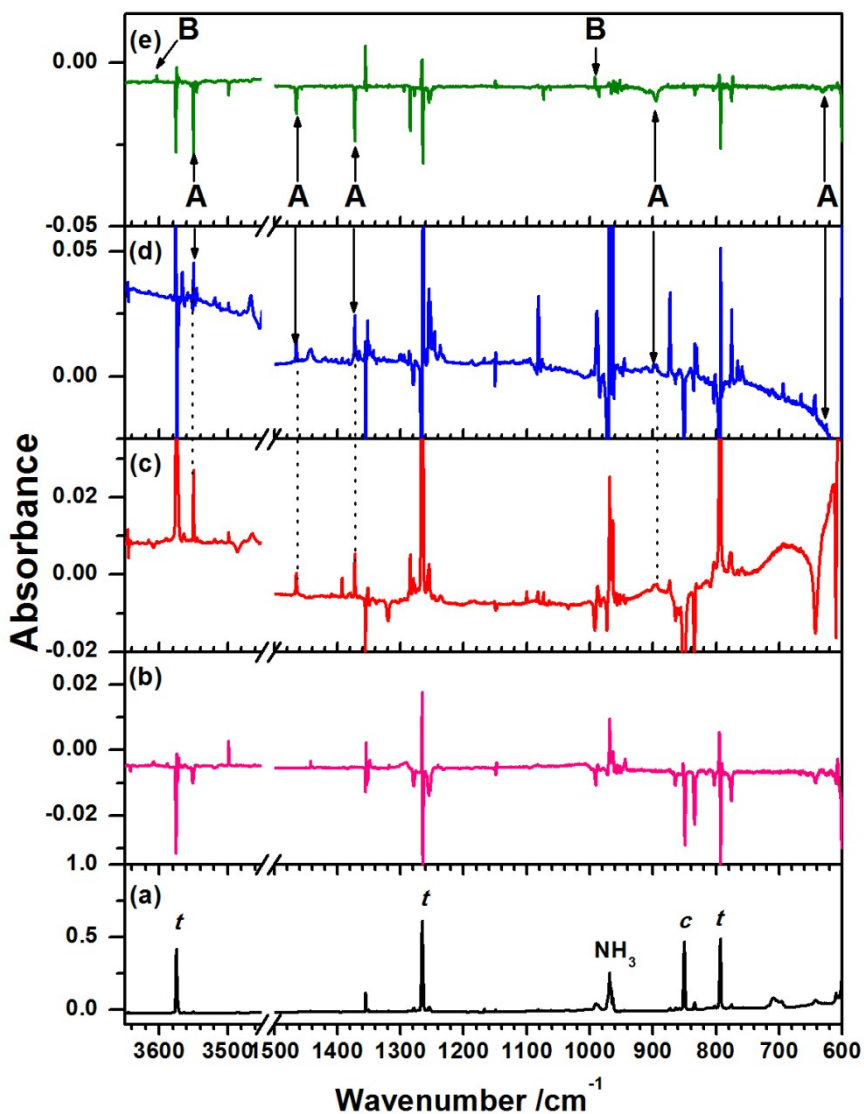


**Fig. S2** Partial spectra of a HONO/NH<sub>3</sub>/Cl<sub>2</sub>/p-H<sub>2</sub> matrix recorded at various stages of an experiment. (a) Absorption spectrum after deposition at 3.3 K for 6 h. (b) Difference spectrum of this matrix upon irradiation with light at 405 nm for 30 min. (c) Difference spectrum of this matrix recorded after IR irradiation for 45 min; (d) Difference spectrum of this matrix recorded 4 h in darkness after irradiation; (e) Difference spectrum of this matrix upon secondary photolysis at 405 nm for 10 min. Lines in groups A [ $\bullet$ ONH(OH)] and B [ $\bullet$ N(OH)<sub>2</sub>] are marked with arrow and labels; *t* and *c* indicate *trans*- and *cis*-HONO, respectively.

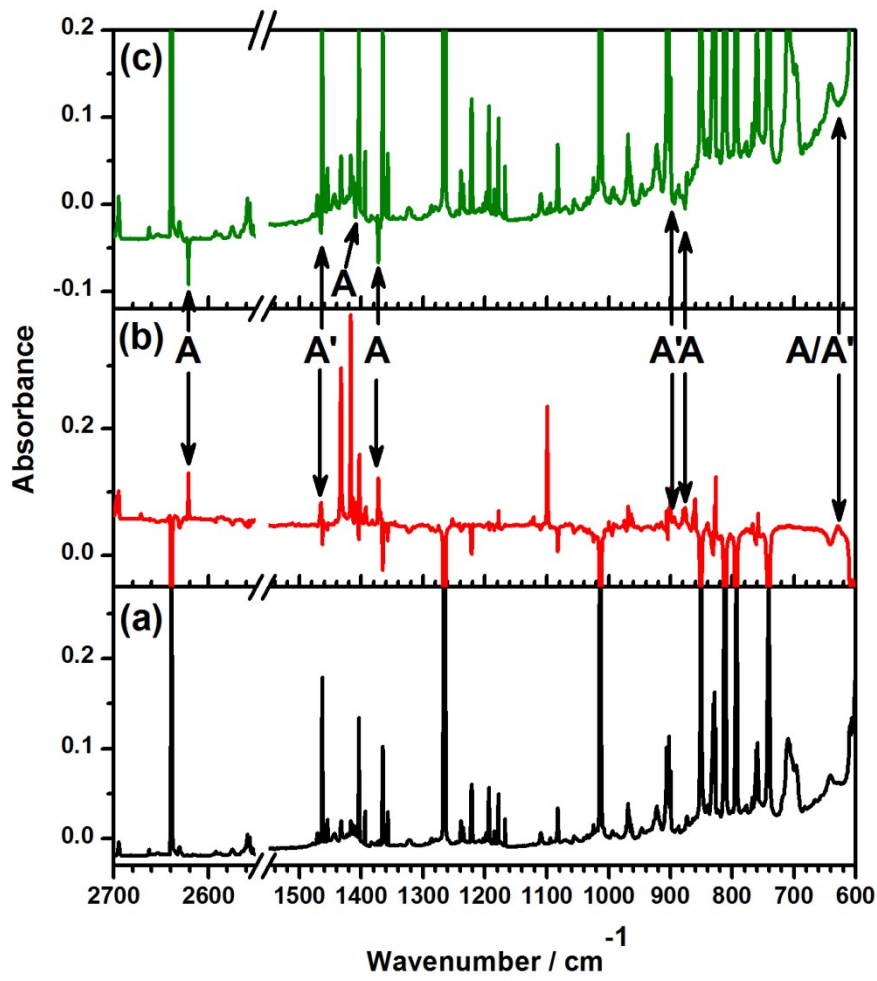


**Fig. S3** Partial spectra of a DONO/NH<sub>3</sub>/p-H<sub>2</sub> matrix recorded at various stages of an experiment. (a) Absorption spectrum after deposition at 3.3 K for 7.5 h. (b) Difference spectrum of this matrix upon irradiation with light at 365 nm for 15 min. recorded 3h after irradiation; (c) Difference spectrum of this matrix upon secondary photolysis at 405 nm for 10 min. Lines in groups A [ $\bullet$ ONH(OD)] and A' [ $\bullet$ ONH(OH)] are marked with arrow and labels.

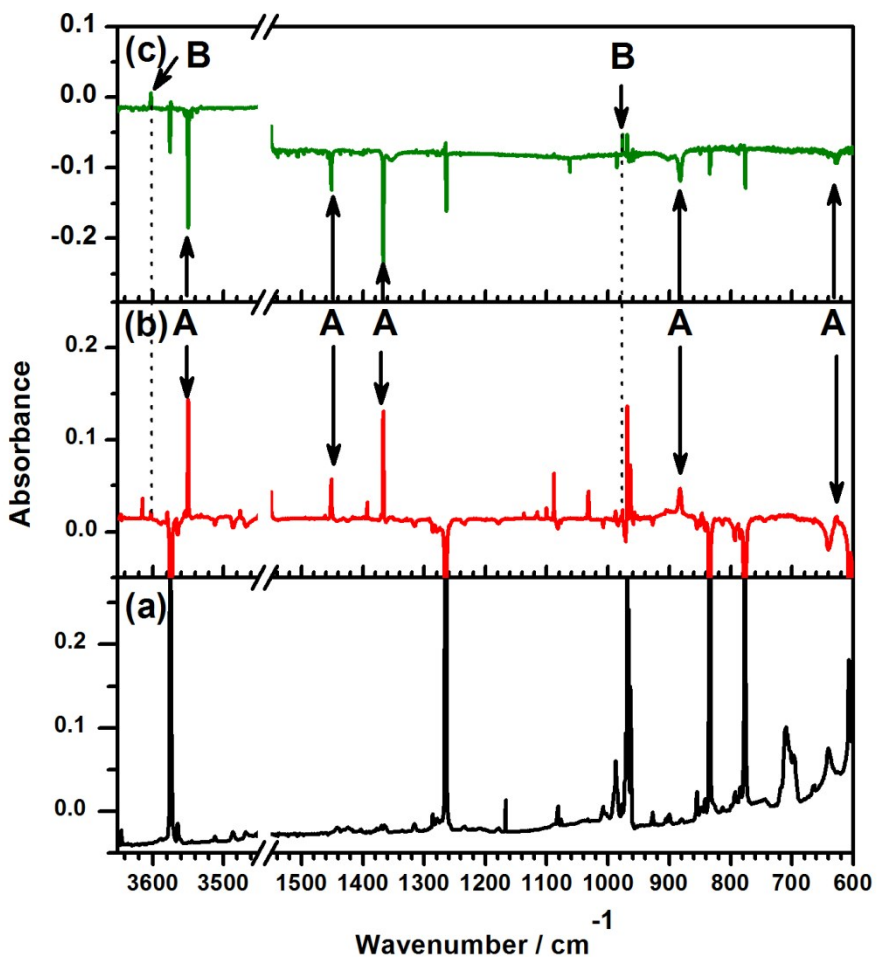


**Fig. S4** Partial spectra of a  $\text{HO}^{15}\text{NO}/\text{NH}_3/\text{p-H}_2$  matrix recorded at various stages of an experiment. (a) Absorption spectrum after deposition at 3.3 K for 8 h. (b) Difference spectrum of this matrix upon irradiation with light at 365 nm for 15 min. recorded 3h after irradiation; (c) Difference spectrum of this matrix upon secondary photolysis at 405 nm for 10 min. Lines in groups A [ $\bullet\text{O}^{15}\text{NH(OH)}$ ] and B [ $\bullet^{15}\text{N(OH)}_2$ ] are marked with arrow and labels.

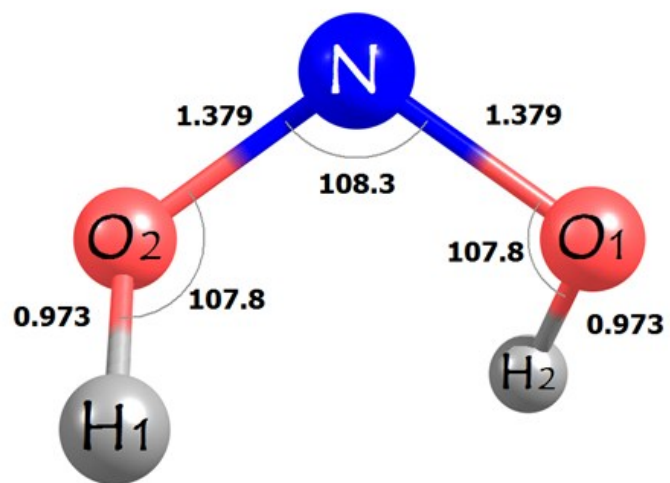


**Fig. S5** Geometries of a less stable conformer of  $\bullet\text{N}(\text{OH})_2$ . The structures were optimized with the B3LYP/aug-cc-pVTZ method; bond lengths are in Å and angles in degree.